NANO LETTERS

2004
Vol. 4, No. 6
1153−1161

Electrochemistry and Electrogenerated Chemiluminescence of CdTe Nanoparticles

Yoonjung Bae,[†] Noseung Myung,[‡] and Allen J. Bard*,[†]

Department of Chemistry and Biochemistry, Center for Nano- and Molecular Science and Technology, Department of Chemistry and Biochemistry, The University of Texas at Austin, Austin, Texas 78712, and Department of Applied Chemistry, Konkuk University, Chungju Campus, Chungju, Chungbuk 380-701, Korea

Received March 30, 2004; Revised Manuscript Received April 9, 2004

ABSTRACT

Differential pulse voltammetry (DPV) of TOPO-capped CdTe nanoparticles (NPs) in dichloromethane and a mixture of benzene and acetonitrile showed two anodic and one cathodic peaks of the NPs themselves and an additional anodic peak resulting from the oxidation of reduced NPs. The electrochemical band gap (∼2.1 eV) between the first anodic and cathodic DPV peaks was close to the value (2 eV) obtained from the absorption spectrum. Electrogenerated chemiluminescence (ECL) of CdTe NPs was highly intense for scans into the negative potential region in dichloromethane. The fact that the ECL peak occurs at about the same wavelength as the band-edge photoluminescence (PL) peak indicates that, in contrast to CdSe NPs, the CdTe NPs as synthesized had no deep surface traps that can cause a substantially red shifted ECL.

1. Introduction. Semiconductor nanoparticles (NPs) have unique electronic properties depending on size and composition that can be probed by spectroscopic and electrochemical measurements. The properties can also be very sensitive to the surface structure because of the large surface-to-volume ratio of NPs compared to the bulk materials.[1]

The electrochemistry of semiconductor NPs can sometimes reveal quantized electronic behavior as well as decomposition reactions upon reduction and oxidation. Our earlier report[2] described the direct correlation of the band gaps of CdS NPs measured by optical and electrochemical methods. The electrochemistry of monolayer-protected gold clusters (MPCs) shows evenly spaced voltammetric peaks that can be attributed to quantized double layer (QDL) charging.[3] The charging capacitance of MPCs of a few aF results in successive current peaks that show the same potential spacing due to single charge additions to the MPCs. However, for semiconductor NPs, such a QDL charging effect has not been well established in general. Si NPs[4] showed cathodic voltammetric peaks due to the QDL charging of particles, but for PbS[5] and CdS[2] NPs, the voltammetric responses were irregular and irreversible because of decomposition of the particles on charge transfer leading to multiple electron-transfer reactions.

The surface structure of NPs also plays a key role in determining the properties of the particles. Unpassivated surface atoms can form electronic traps for electrons and holes that affect the luminescence processes. Figure 1 shows pathways of photoluminescence (PL) of a NP. In the core, there is excitonic radiative emission near the same wavelength as the absorption. On the surface, the surface traps formed within the band gap can cause luminescence at significantly longer wavelengths and act as nonradiative recombination centers that lower the efficiency of photoluminescence. Thus, the passivation of surface traps is very important to obtain a highly efficient luminescence with a narrow emission line width. This passivation can be accomplished by capping the particle surface with an organic agent or shell of a larger band gap semiconductor. In this report, we used trioctylphosphineoxide (TOPO) to passivate the surface of CdTe NPs.[6] Recently we demonstrated that the electrogenerated chemiluminescence (ECL) of NPs is much more sensitive to their surface electronic structure than the PL, which is mainly characterized by the bulk electronic structure.[4,7,8] For example, Si[4] and CdSe[7] NPs showed an ECL emission that was substantially red shifted from the band-edge PL; this was attributed to surface state emission. On the other hand, CdSe NPs that were well-passivated with a shell of ZnSe (CdSe/ZnSe core shell NPs) showed a large ECL peak at the wavelength of band-edge PL.[8]

* Corresponding author.
[†] The University of Texas at Austin.
[‡] Konkuk University.

10.1021/nl049516x CCC: $27.50
Published on Web 04/27/2004

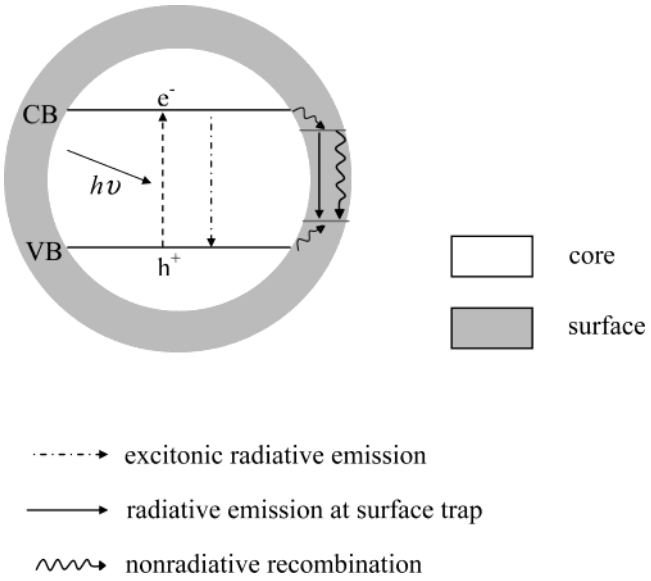

Figure 1. Diagram of photoluminescence of a nanoparticle in the core and on the surface.

We describe here the electrochemistry and ECL of 4 nm diameter CdTe NPs. CdTe is a useful group II−IV compound semiconductor that has been used in photovoltaic cells and electrooptic modulators, because its band gap (1.5 eV at 300 K) is in the visible region and its optical absorption coefficient is high.[9] In particular, we determined the electrochemical band gap of the particles and explain the voltammetric peaks observed in solution. Because of the close correspondence of the ECL and PL spectra, we suggest that the tellurium surface sites are passivated as synthesized.

2. Experimental Section. *2.1. Chemicals and Apparatus.* Cadmium acetate hydrate (99.99%), tellurium (200 mesh, 99.8%), trioctylphosphine (TOP; tech. 90%), and trioctylphosphineoxide (TOPO; tech. 90%) were obtained from Aldrich and were used without further purification. Dichloromethane, acetonitrile, benzene (all anhydrous, 99.8%, Aldrich), tetra-*n*-butylammonium hexafluorophosphate ($TBAPF_6$; Fluka, >99.0%), tetra-*n*-butylammonium perchlorate (TBAP; Fluka, >99.0%), methanol (Fisher, certified A. C. S.), and chloroform (Fisher, certified A. C. S.) were used as received.

UV−vis absorption and PL spectra were measured with a Milton Roy Spectronic 3000 array spectrophotometer and PTI fluorometer, respectively, with rhodamine6G used as a standard to determine the relative PL quantum efficiency. Transmission electron microscopy (TEM) was performed on a Philips 208 microscope with the sample prepared by dropping a dilute particle solution on carbon film coated gold grids.

For the electrochemistry and ECL experiments, the particle solution was vacuum dried and the resulting powder was dissolved in dichloromethane or a 5:1 (v/v) benzene/acetonitrile mixture containing TBAP or $TBAPF_6$ as a supporting electrolyte. The solution was placed in an airtight cell inside a nitrogen filled drybox (MB200MOD-1-I, mBRAUn, Germany) and the cell was closed and taken outside the drybox for the experiments. Electrochemical experiments were carried out with a potentiostat (model 660, CH Instruments, Austin, TX) and Autolab electrochemical workstation (Eco Chemie, Netherlands) with a three-electrode system: a Pt disk working electrode, a Pt wire counter electrode, and an Ag wire quasi-reference electrode. The cell potential was referenced to the standard calomel electrode (SCE) by using Fc/Fc^+ couple where the potential of this couple in any solvent is assumed to be the same as measured in acetonitrile, i.e., 0.342 V vs SCE.[10] Background potential scans in electrolyte solution in the absence of CdTe NPs were obtained in all cases to determine which peaks could be attributed to impurities. ECL transients were measured using an Autolab electrochemical workstation coupled with a photomultiplier tube (PMT, Hamamatsu R4220p), and ECL spectra were obtained by applying a potential program with a PAR model 175 universal programmer and model 173 potentiostat-galvanostat and recorded on a charge coupled device (CCD) camera (CH260, Photometrics, Tucson, AZ) cooled below −104 °C with liquid N_2 and a grating monochromator (Chemspec 100S, American Holographics Inc., Littleton, MA). The recorded spectra were calibrated with an Hg−Ar vapor lamp.

2.2 Synthesis of CdTe Nanoparticles. CdTe NPs were synthesized according to the procedure developed by Peng and co-workers.[6] The tellurium precursor solution was prepared by loading 0.0664 g (0.52 mmol) of tellurium powder and 2 g (5.4 mmol) of TOP in a glass vial inside a nitrogen filled drybox and heating it at 210 °C for ∼3 h to dissolve the tellurium in the TOP outside the drybox. The heating was maintained until the resulting solution showed a greenish-yellow color. If the heating was continued beyond this point, the solution color changed to dark yellow; this solution would not yield an optically clear NP solution but rather a blackish precipitate as the product. The cadmium precursor solution was prepared by mixing 0.0922 g (0.4 mmol) of cadmium acetate hydrate and 8 g (20.7 mmol) of TOPO in a 25 mL three-neck round-bottom flask and increasing the temperature to 150 °C under an argon atmosphere. The mixture was kept at this temperature for 1 h and the colorless solution showed a pale yellow color after this time. This solution was then heated to 310 °C and the color changed to dark yellow. The cadmium precursor solution was held at this temperature and the tellurium solution, cooled to room temperature, was injected quickly into the reaction flask, stirred vigorously, and the heat was removed immediately. The color of the solution abruptly changed from dark yellow to reddish black. When the resulting solution cooled to ∼150 °C, the solution color changed to blood-red, which was the final product color. 10 mL of chloroform was added at 60 °C.

The NPs dispersed in the resulting solution were precipitated in methanol and collected by centrifugation and decantation. The precipitate was dissolved in chloroform and centrifuged. The purified solution was used for spectroscopic measurements or vacuum-dried for electrochemical and ECL measurements.

3. Results and Discussion. *3.1 Characterization of CdTe Nanoparticles.* The absorption and PL spectra of CdTe NPs are shown in Figure 2. The band gap from the absorption

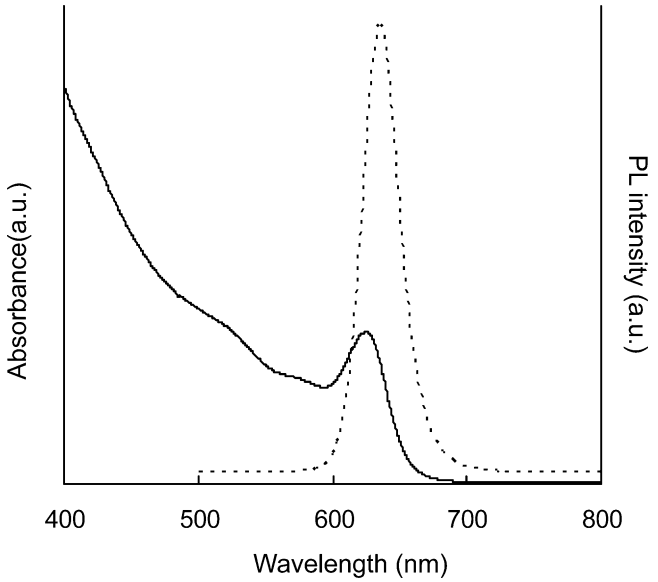

Figure 2. Absorption (solid line) and PL (dashed line, $\lambda_{ex} = 480$ nm) spectra of CdTe NPs in $CHCl_3$.

peak is 2.0 eV (625 nm) and is shifted to higher energy from the band gap of bulk CdTe (1.5 eV),[9] representing the quantum size effect of the NPs.[1] A particle size of 3.9 nm is estimated from this spectrum, based on the first absorption peak wavelength.[11] From TEM measurements, the particle size was 4.0 ± 0.2 nm, demonstrating a narrow size distribution.

The PL shows a peak at 635 nm and the quantum yield is ~3% relative to rhodamine6G at room temperature. In particular, the PL went down to the background level at longer wavelengths without any PL tail, suggesting no significant luminescence from surface traps. In general, PL of NPs at substantially longer wavelength from the band-edge PL is assigned to surface trap emission.[1f,12] For example, Wuister and co-workers[12] reported two PL peaks of trioctylphosphine/dodecylamine-capped CdTe NPs, one corresponding to band-edge emission and the other from trap emission. However, after modification of the capping groups, the band-edge PL was enhanced and showed no surface trap emission. This property (no observable surface trap emission of TOPO-capped CdTe NPs) will be referred to again to support the result of ECL.

In addition, the concentration of NPs was estimated as 40 μM by using the number of CdTe units (493 CdTe units) in a NP of this size and assuming that all of the cadmium precursor was consumed in the NP formation process. The total number of atoms in a particle was calculated by multiplying the number of atoms per unit lattice volume (8 atoms are contained in a cubic lattice with a spacing of 6.477 Å)[13] by the volume of a spherical NP of radius 20 Å. The particle consists of approximately 987 atoms (493 CdTe units). The concentration of NPs was calculated based on moles of cadmium precursor and total volume of resulting solution, 20 mL. The estimated concentration of 40 μM is, however, about twice that of the value of 19 μM obtained from absorption measurements using an extinction coefficient of 4 nm size CdTe NPs ($\epsilon = 1.9 \times 10^5$ cm^{-1} M^{-1}).[11] Thus,

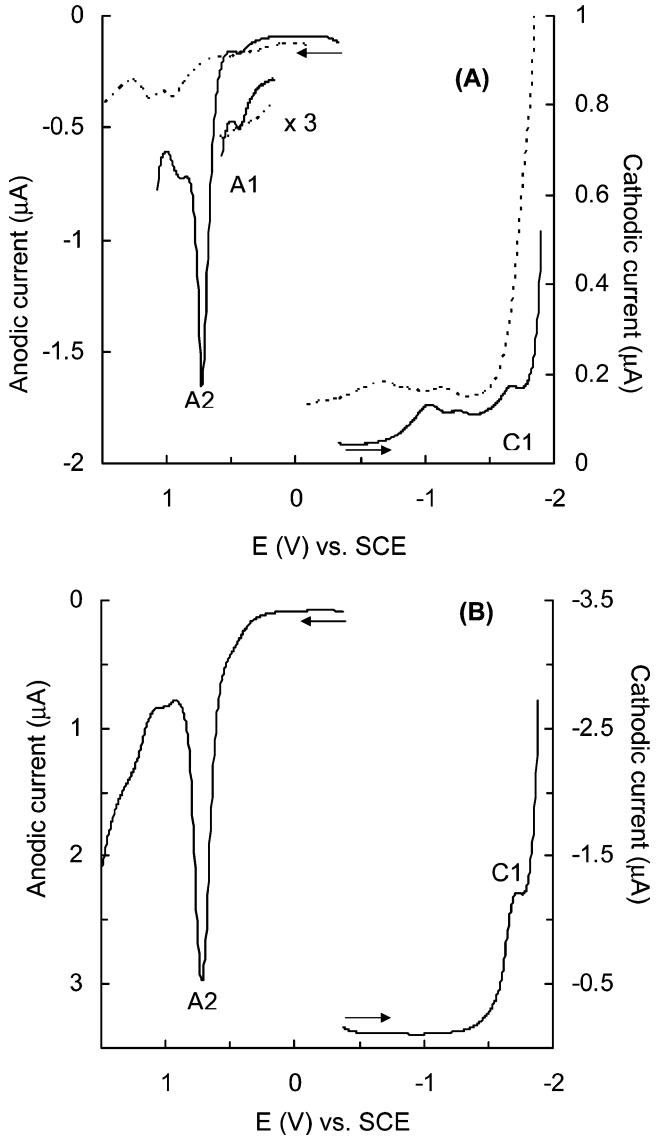

Figure 3. Differential pulse voltammograms of two different batches of CdTe NPs at a 0.06 cm^2 Pt working electrode with scan toward positive or negative potentials, scan rates of 10 mV/s and pulse amplitude of 50 mV. The arrows indicate the starting potential and scan direction. (A) 9.6 μM CdTe NPs in 5:1 (v/v) benzene/acetonitrile containing 0.1 M TBAP. The current value of peak A1 is magnified three times and dotted lines are background signal from supporting electrolyte solution. (B) 32 μM CdTe NPs in CH_2Cl_2 containing 0.1 M $TBAPF_6$.

about half of the cadmium precursor participated in the formation of the NP.

3.2. Electrochemistry. As with other semiconductor NPs, obtaining good electrochemistry is difficult, because the concentrations of the TOPO-capped CdTe NPs in typical solvents, like CH_2Cl_2, benzene and THF are small (typically about 10 to 30 μM) and differential pulse voltammetry (DPV) is often used to obtain a good signal over background. Figure 3 shows DPVs of two different batches of CdTe NPs. In Figure 3a, in a 5:1 (v/v) benzene/acetonitrile mixture as a solvent, three anodic peaks (A1 and A2 at 0.45 and 0.73 V with potential spacing of 0.28 V and an additional peak at 0.9 V) were observed in the positive potential scan. Three cathodic peaks (C1 at −1.68 V and two other peaks at −1.0

Table 1. Diffusion Coefficients of TOPO-Capped CdTe NPs

	D_{NP} (cm^2/s) from DPV peaks[a]		D_{NP} (cm^2/s) from Einstein-Stokes eq.[b]
	A1	C1	
Figure 3A	1.3×10^{-7}	2.0×10^{-7}	1.4×10^{-6}
Figure 3B		2.0×10^{-6}	1.9×10^{-6}

[a] DPV peak current, $(\delta i)_{max} = (nFAD_o^{1/2}C_o^*(1-\sigma)/(1+\sigma))/(\pi^{1/2}(\tau-\tau')^{1/2})$[23] where pulse width $(\tau - \tau')$ is 0.05 s, $\sigma = \exp(nF\Delta E/2RT)$ where pulse height ΔE is 50 mV and assumed single charge ($n = 1$) reaction. [b] Einstein-Stokes equation,[3(b)] $D = k_BT/6\pi\eta r_H$, where k_B is the Boltzmann constant (1.38×10^{-23} J/K), T is the absolute temperature, η is solvent viscosity ($\eta_{benzene,\ 300\ K} = 0.5883$ cP, $\eta_{ACN,\ 300\ K} = 0.3548$ cP, $\eta_{CH2Cl2,\ 300\ K} = 0.4060$ cP),[24] and r_H is the hydrodynamic radius of species ($r_H \approx r_{CdTe\ NP} + d_{TOPO} = 2$ nm + 0.7 nm, the length of TOPO monolayer, d_{TOPO}, are adapted from experimental results using electrostatic force microscopy (EMF)[25]).

and −1.24 V) appear in the negative potential scan direction. The first anodic peak (A1), as discussed later, is characteristic of a one-electron reaction and could sometimes not be distinguished well from the background, as shown in Figure 3b, even in the same batch of particles in the same electrolyte solution. The third anodic peak around 0.9 V and two cathodic peaks at potentials positive of −1.68 V were not reproducible and are probably due to impurities in the NP preparation or reduction of residual oxygen. The electrochemical band gap between the first cathodic (C1) and anodic (A1) peaks from Figure 3A is 2.13 V, which is close to the value of 2 eV obtained spectroscopically. Similarly, in Figure 3B, the electrochemical band gap is ~2 eV if the positive onset point or the shoulder near ~0.45 V is taken as the first anodic current peak. Recently, Gao and co-workers[14] reported voltammetric current peaks of thioglycolic acid-stabilized CdTe NPs around −1 and +1 V (vs Ag|AgCl) in aqueous solution. Similar voltammetic behavior was observed by Greene and co-workers[15] from a solid film of dimethyldioctadecylammonium-stabilized CdTe NP monolayer. They reported an electrochemical band gap that correlated with the optical value as well as anodic current peaks located at potentials inside the valence band edge, which were explained by hole injection into the surface traps of the particles.

To get some quantitative feeling for the observed wave heights, we estimated the diffusion coefficient of the NPs (D_{NP}) from the DPVs by assuming a single electron reaction and compared it with the value estimated from the Stokes−Einstein equation (Table 1). The D_{NP} measured from A1 and C1 in Figure 3A was approximately 10 times smaller than the expected value. This would indicate that the electron-transfer reaction of A1 and C1 would involve less than one electron, which is unreasonable. However, the D_{NP} measured from C1 in Figure 3B is similar to the expected value and suggests a single electron reaction per NP in C1. The small D_{NP} obtained from Figure 3A may be caused by uncertainty in the estimation of the small current values associated with the electron-transfer reaction in the presence of the large background current in the DPV measurement at the small NP concentration or an error in the concentration estimation.

The large reproducible peak, A2, which is 10 to 15 times larger than A1 and C1, could result from adsorbed species on the platinum surface, other components contained in the NP solution, or multicharge (hole) injection into the NPs. To investigate the possibility of the wave being caused by a species formed by reduction of the CdTe NPs, DPVs were taken starting at different initial potentials. Figure 4a shows DPVs with initial potentials of −0.5 V (solid line) and 0.5 V (dotted line), respectively. The same peak current for A2 was found with both initial potentials, so this peak probably does not involve species of the NPs reduced below −0.5 V. To investigate the possibility of adsorption, CVs at different scan rates were obtained as shown in Figure 4b. The linear relationship between the peak current and the $v^{1/2}$ shows A2 is mainly from diffusion of particles in solution, with no appreciable contribution from an adsorbed species. The sample, as synthesized, contains capped CdTe NPs, residual precursor and capping agents, and impurities from the TOP

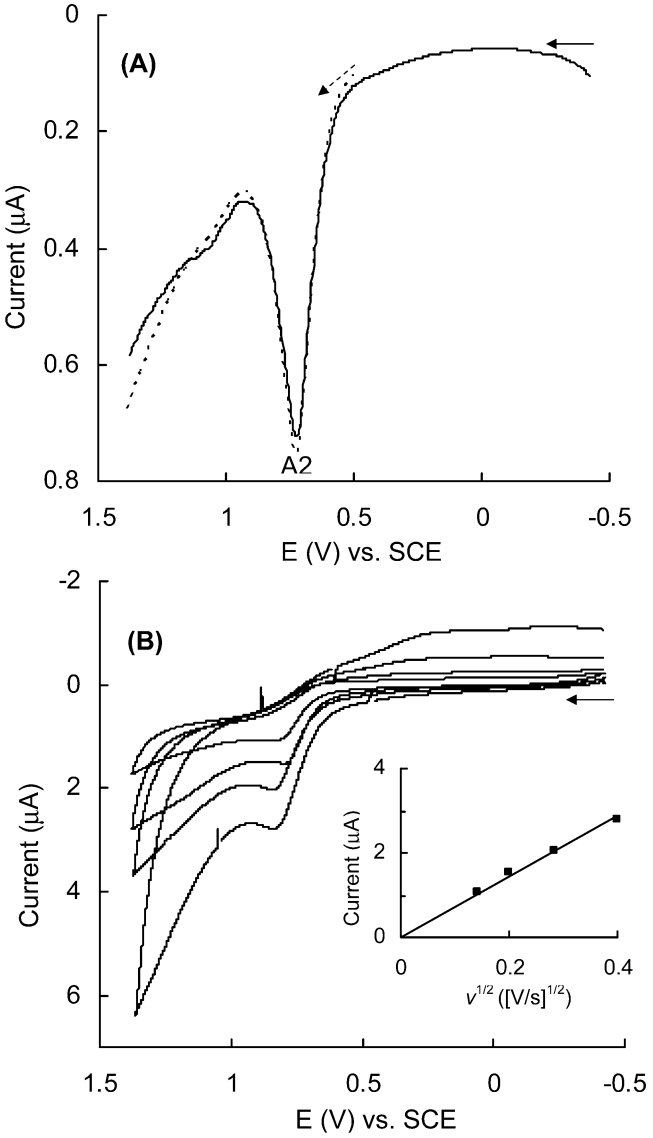

Figure 4. (A) Differential pulse voltammograms with different staring potentials, −0.5 and 0.5 V, (10 mV/s scan rate and 50 mV pulse amplitude) and (B) cyclic voltammograms with different scan rates (0.02, 0.04, 0.08, and 0.16 V/s) and scan toward positive potentials of 9.1 μM CdTe NPs in 5:1 (v/v) benzene/acetonitrile containing 0.1 M TBAP at a 0.03 cm^2 Pt working electrode. Inset shows linear relationship between peak current around 0.7 V and $v^{1/2}$.

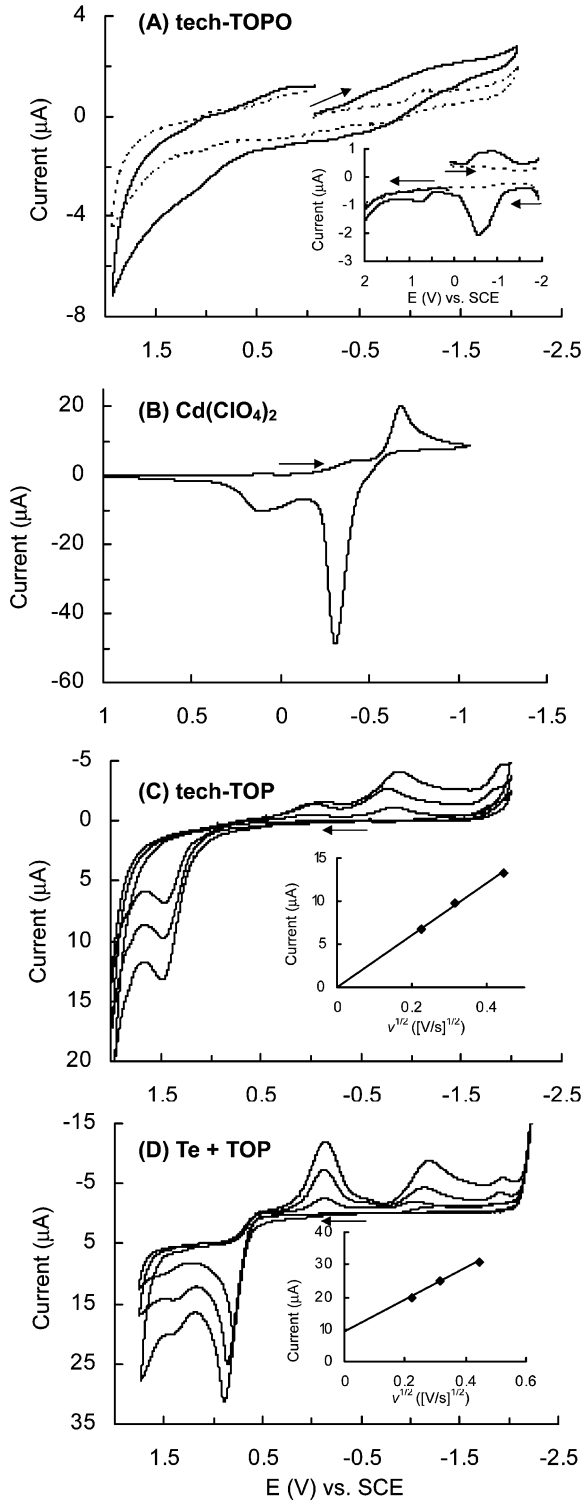

Figure 5. Cyclic voltammograms of each precursor and capping agent solution. (A) 4.1 mM tech-TOPO in 0.1 M TBAP + acetonitrile with scan rates of 50 mV/s, (inset: differential pulse voltammograms of ~11 mM TOPO, dotted lines are background signal from supporting electrolyte solution). (B) ~1.6 mM $Cd(ClO_4)_2$ in 0.1 M TABP + acetonitrile with scan rates of 50 mV /s. (C) ~1.4 mM tech-TOP in 0.1 M $TBAPF_6 + CH_2Cl_2$ with scan rates of 50, 100, and 200 mV/s (inset: plot of peak current around 1.5 V versus $v^{1/2}$). (D) Te + TOP (~0.2 mM Te and ~2.9 mM TOP) in 0.1 M $TBAPF_6 + CH_2Cl_2$ with scan rates of 50, 100, and 200 mV/s, (inset: plot of peak current around 0.8 V versus $v^{1/2}$), at a 0.03 or 0.04 cm^2 Pt working electrode. The arrows indicate the starting potential and scan direction.

and TOPO solutions. Other components, except for the capped NPs, should largely dissolve in methanol during the purification step and probably are not at a high enough concentration to produce this wave. We examined the electrochemical behavior of each precursor and capping agents to see if any current flows at a similar potential of peak A2. Cadmium and tellurium precursors were prepared by following the same procedure as that used in the NP synthesis. Both precursor solution and technical grade TOPO were vacuum-dried, and technical grade TOP was used as stored in the drybox and dissolved in an appropriate solvent for electrochemical studies as shown in Figure 5. The CV of tech-TOPO does not show apparent current peaks corresponding to the TOPO itself in the potential range of +2 to −2 V. The DPVs of TOPO in the inset show two broad cathodic peaks around −0.6 and −1.1 V, which could result from impurities in TOPO such as dioctylphosphinic acid or monooctylphosphonic acid,[16] and an additional anodic peak resulting from the oxidation of reduced species. Figure 5b shows the reduction of cadmium ion at −0.7 V and the anodic stripping at −0.3 V where cadmium perchlorate was used to observe the electrochemical behavior of cadmium ion in place of cadmium acetate because of the insolubility of cadmium acetate in organic solvents. In the TOP solution, as shown in Figure 5c, an anodic current flows around 1.5 V and reduction of the oxidized species occurs at −0.02 and −0.86 V. These two cathodic current peaks are observed only after the potential scans to positive voltages around 1.5 V. The anodic peak current probably represents oxidation of TOP in terms of the TOP concentration and it is proportional to the square root of scan rate. In Figure 5d, tellurium in a TOP solution shows an anodic peak around 0.8 V and another peak at ~1.4 V, which is quite similar to the anodic peak in a TOP solution. Two cathodic peaks are also observed only after positive potential scans. Interestingly, the anodic peak around 0.8 V is 20 or 10 times larger (depending on the number of electrons assumed in the electrode reation, 1 or 2) than the expected value from the concentration of tellurium, ~0.2 mM. From the electrochemistry of each precursor and capping agent, peak A2 in Figures 3 and 4 seems to be caused by oxidation of tellurium species of NPs. This phenomenon may result from instability of the oxidized particle.

When the potential was scanned from negative values at or beyond wave C1 to positive potentials, an additional anodic current peak appeared as shown in Figure 6. The additional peak was found reproducibly around 1.1 V. This peak clearly results from oxidation of reduced species which remained on the platinum surface. Simply, by comparison with the electrochemistry of capping agents, this additional peak seems to result from the oxidation of TOP.

The electrochemistry explained as the oxidation of tellurium species and reductively produced species may become different in more completely passivated NPs or particles capped with other capping agents instead of TOPO and TOP. The effect of different ligands on the electrochemistry of CdTe NPs will be studied so that more quantitative studies can be done at an increased NP solubility.

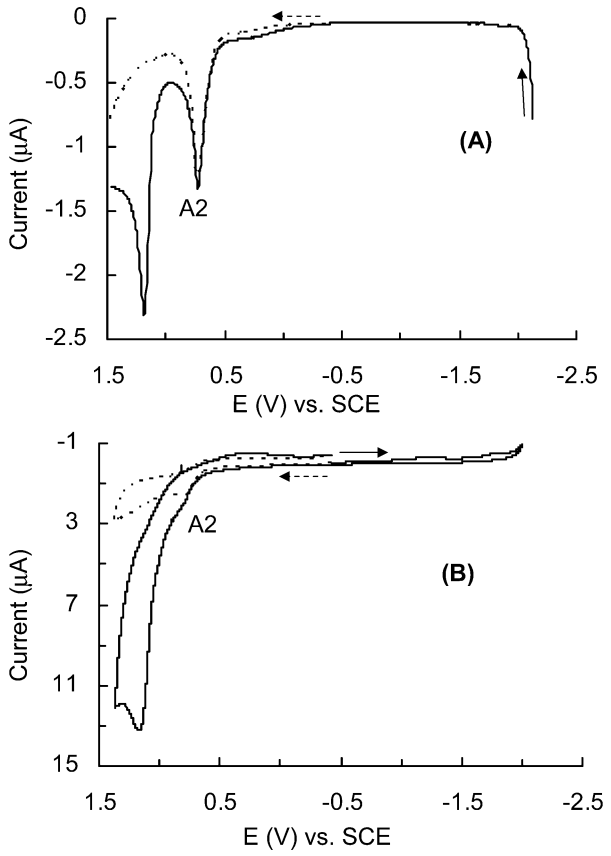

Figure 6. (A) Differential pulse voltammograms with different starting potentials of 8.4 μM CdTe NPs in 5:1 (v/v) benzene/acetonitrile containing 0.1 M $TBAPF_6$ at a 0.03 cm^2 Pt working electrode with scan rates of 10 mV /s and pulse amplitude of 50 mV. (B) Cyclic voltammograms with different scan directions of 9.1 μM CdTe NPs in 5:1 (v/v) benzene/acetonitrile containing 0.1 M TBAP at a 0.03 cm^2 Pt working electrode and scan rates of 0.04 V/s.

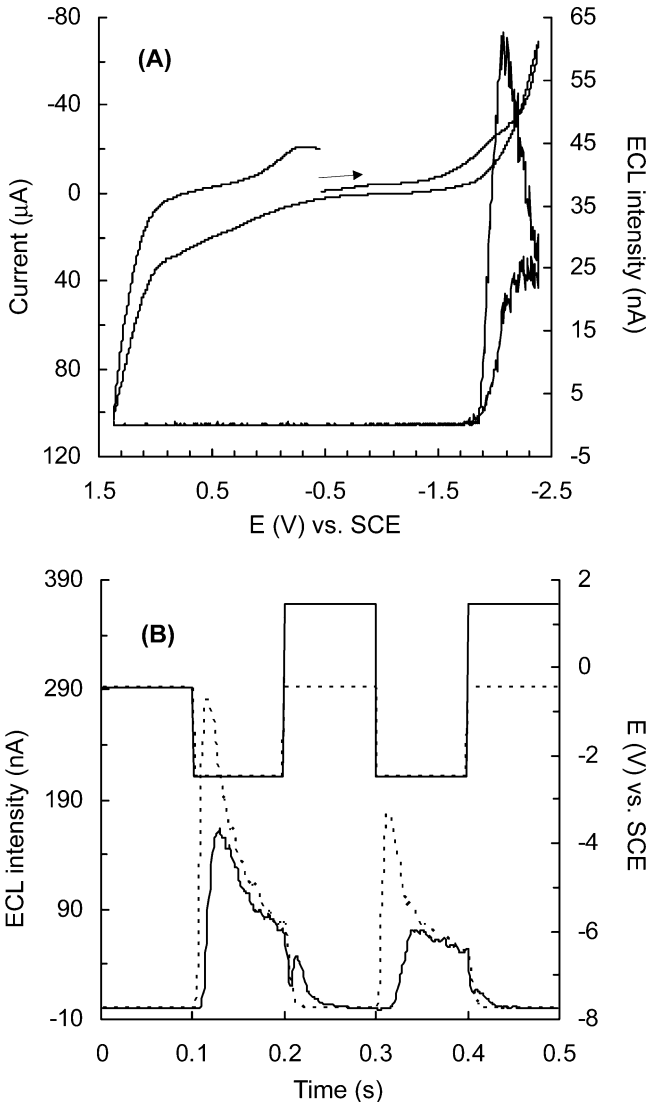

Figure 7. (A) Cyclic voltammogram and the corresponding ECL potential curve (scan rate: 1V/s) and (B) ECL transients (lower curves) by stepping potential (upper curves) between −2.46 and +1.44 V (solid line) or half potential between −0.46 and −2.46 V (dotted line) of ∼7 μM CdTe NPs in CH_2Cl_2 containing 0.1 M $TBAPF_6$ at a 0.06 cm^2 Pt working electrode.

3.3. Electrogenerated Chemiluminescence. Figure 7 shows an ECL-potential curve and transients of CdTe NPs in dichloromethane containing 0.1 M $TBAPF_6$. As the potential is scanned from zero to −2.46 V (vs SCE) at 1 V/s scan rate, as shown in Figure 7a, significant ECL signal is detected around −1.85 V, which is slightly negative of the first cathodic DPV peak potential (see Figure 3) and it shows a large peak at more negative potential. However, in a reverse potential scan, ECL is not observed at positive potential region. In Figure 7b, the ECL transients are measured by applying 10 Hz potential steps between −2.46 and +1.44 V (solid line). A large ECL signal is detected at the first negative potential step and a much smaller ECL signal at the subsequent positive potential. The latter can be explained by electron transfer reaction between reduced and oxidized NPs. This small ECL signal is not often detected even in ECL transients. The former ECL observed at the first negative potential region is not explained with annihilation of redox species of NPs because there are only reduced particles without the oxidized ones acting as an electron acceptor. Rather, a larger ECL signal is still observed by applying negative potential steps from −0.46 to −2.46 V in Figure 7b (dotted line). There might be another oxidized species (Ox) to accept an electron from the anion particle radicals and to form the emitter.[17]

$$(CdTe)_{NP}^{-\bullet} + Ox \rightarrow (CdTe)_{NP}^{*} + \text{products} \qquad (1)$$

(Here, we assume that NPs in bulk solution are neutral.) The oxidant (Ox) can come from supporting electrolyte, $TBAPF_6$, or dichloromethane solvent. In a different supporting electrolyte, 0.1 M TBAP−CH_2Cl_2 system, significant ECL signal at the first negative potential was still observed. However, in a different solvent, a mixture of benzene and acetonitrile as shown in Figure 8, ECL signal is 30 times lower at the first negative potential, which can be attributed to some impurities in the cell. These results suggest that the large ECL at the first negative potential in Figure 7 might result from the oxidized form from the dichloromethane solvent. Ushida and co-workers[18] revealed that $CH_2Cl^{\bullet}$ radicals

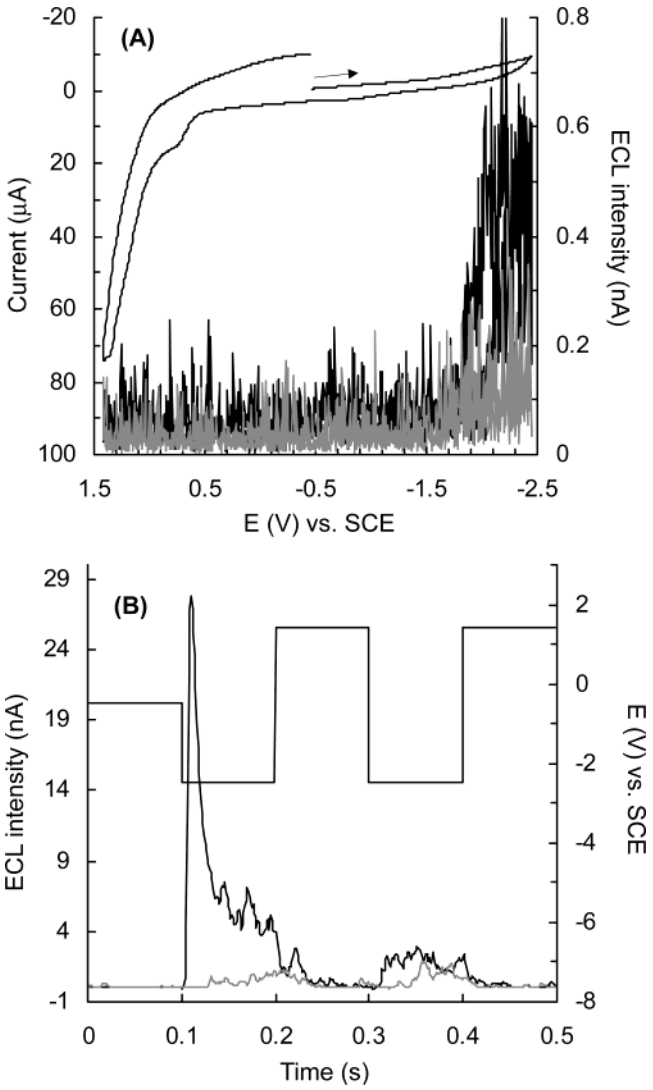

Figure 8. (A) Cyclic voltammogram and the corresponding ECL potential curves (scan rate: 0.1V/s) and (B) ECL transients (lower curves) by stepping potential (upper curves) between −2.46 and +1.44 V of ∼14 μM CdTe NPs in 5:1 (v/v) benzene/acetonitrile containing 0.1 M $TBAPF_6$ at a 0.1 cm^2 Pt working electrode. Gray line shows background ECL signal from supporting electrolyte solution.

produced under irradiation of CH_2Cl_2 play a role as an electron acceptor to oxidize aromatic hydrocarbons. Based on this reference, we propose $CH_2Cl^{\bullet}$ as an oxidant in our system. The reduced CH_2Cl_2, $CH_2Cl_2^{-\bullet}$, decomposes into $CH_2Cl^{\bullet}$ and Cl^-, and the oxidant, $CH_2Cl^{\bullet}$, accepts an electron from reduced NP to form the emitting state.

$$CH_2Cl_2 + e^- \rightarrow CH_2Cl_2^{-\bullet} \rightarrow CH_2Cl^{\bullet} + Cl^- \quad (2)$$

$$(CdTe)_{NP}^{-\bullet} + CH_2Cl^{\bullet} \rightarrow (CdTe)_{NP}^{*} + CH_2Cl^- \quad (3)$$

ECL resulting from mechanisms (3) is possible only when the reaction enthalpy ($\Delta H°$) characterized by the redox reaction is larger than the first excited singlet state energy, E_s.[19]

$$-\Delta H° = E_a° - E_c° - 0.1\ \text{eV} > E_s \quad (4)$$

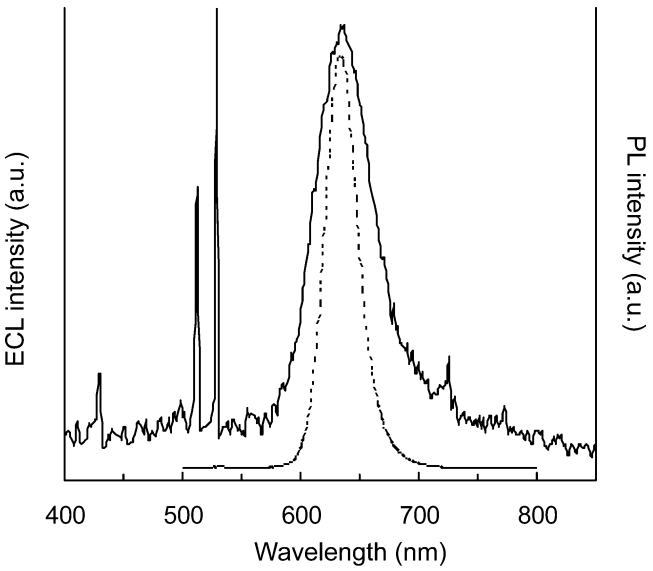

Figure 9. ECL spectrum (solid line) obtained by stepping potential between −2.3 and +2.3 V (vs Ag wire) at 10 Hz with an integration time of 20 min of ∼7 μM CdTe NPs in CH_2Cl_2 containing 0.1 M TBAP at a 0.1 cm^2 Pt working electrode. Dotted curve is PL spectrum to compare with ECL spectrum.

Table 2. Difference between PL and ECL Position of Si, CdSe, and CdTe NPs

	λ_{PL} (nm)	λ_{ECL} (nm)	$\lambda_{ECL} - \lambda_{PL}$ (nm)
Si NPs[4]	365	640	275
CdSe NPs[7]	545	740	195
CdTe NPs	635	638	3

E_s of CdTe NPs is 1.95 eV from the PL measurement in Figure 2. In mechanism (3), i.e., the co-reactant scheme, we assume that oxidation potential of CH_2Cl^- to $CH_2Cl^{\bullet}$ might be larger than 0.4 V (vs SCE) to form the emitting state based on the reduction potential of NPs (∼−1.68 V vs SCE). In addition, annihilation of NP ions is possible thermodynamically because the difference in voltammetric peak potentials ($E_a° - E_c°$) is ∼2.13 eV. However, from Figures 7 and 8, most of the ECL results from the reaction between reduced NPs and CH_2Cl_2 solvent as a co-reactant.

3.4. Surface States. Recently, this research group has reported that the comparison between ECL and PL of NPs is a good way to investigate if the NPs have significant surface traps, because ECL is mainly characterized by surface state transitions as compared with PL.[4,7,8] Si[4] and CdSe[7] NPs showed a substantially red shifted ECL peak due to surface trap emission as shown in Table 2. It means the NPs have surface traps by incomplete passivation of NP surface with capping agents. However, more completely passivated CdSe NPs with a shell of ZnSe, CdSe/ZnSe NPs showed a small ECL peak at a wavelength substantially red shifted and a much larger ECL peak around the wavelength of PL.[8]

In contrast, CdTe NPs show a unique ECL spectrum in Figure 9. That ECL peak at 638 nm is very close to the PL maximum at 635 nm, which was obtained by stepping potential between −2.3 and +2.3 V (vs Ag wire) at 10 Hz in dichloromethane solvent. The same ECL peak position

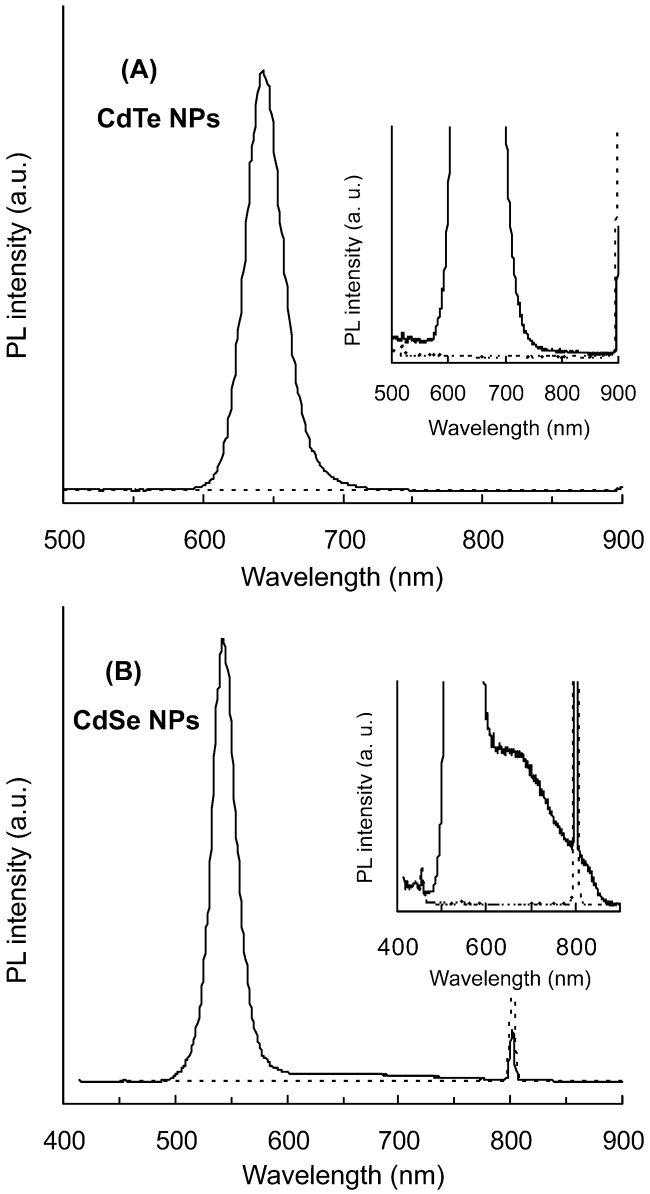

Figure 10. PL spectra of (A) CdTe NPs (λ_{ex} = 450 nm) and (B) CdSe NPs (λ_{ex} = 400 nm) dispersed in $CHCl_3$. Insets show magnified PL spectra in the range of low intensity and dotted lines represent background PL from $CHCl_3$.

was observed by stepping half potential between zero and −2.3 V (vs Ag wire). The result of Figure 9 suggests the CdTe NPs as synthesized have no deep surface traps causing luminescence at longer wavelength. Even though the CdTe NPs were synthesized with the same procedure used in CdSe NPs with TOPO capping agent,[6,7] they show more completely passivated surface states than CdSe NPs based on the ECL results.

To support the superior surface passivation of CdTe NPs, we investigated PL tails at longer wavelength than the wavelength of band-edge PL. As shown in Figure 10, the PL of CdTe NPs decreases to background levels without tails at longer wavelength, but CdSe NPs give a small and very broad PL tail. Yet, it is not clear why CdTe NPs have a superior degree of surface passivation. Surface studies of TOPO-capped CdSe NPs have reported that most of the TOPO capping agent binds to cadmium sites on the surface and most selenium surface sites are unbound because of the basic character of TOPO.[20,21] As a result, unpassivated selenium or tellurium sites on the surface have been proposed as surface hole traps. We assume the tellurium surface sites can be more easily passivated by a surrounding component than selenium surface sites based on the ECL spectra of both NP systems. Very recently, Borchert and co-workers[22] reported the surface structures of thioglycolic acid-capped CdTe NPs with different PL efficiency. They proposed that, in highly luminescent CdTe NPs, sulfur of thiol ligands replaces tellurium surface atoms and binds to cadmium atoms more effectively. On the other hand, in lowly luminescent NPs, most of tellurium surface atoms exist as traps decreasing the PL efficiency in two forms, unpassivated and oxidized tellurium. Based on this report, we consider that the tellurium surface atoms may exist as oxidized forms or be replaced by TOPO ligands or oxygen. In the former case, tellurium atoms can react with oxygen and form the oxidized surface states more easily than selenium atoms according to their electronegativity trends. Otherwise the latter case, where TOPO ligands or oxygen replace the tellurium surface sites and bind to cadmium atoms, can be considered as a factor. However, from a low PL efficiency of TOPO-capped CdTe NPs, ∼3%, the first assumption is more reasonable to explain their superior surface passivation. Even the oxidized tellurium surface site may act as a luminescent quencher producing low efficiency of PL,[22] it can prevent the luminescence at longer wavelength compared to unpassivated tellurium sites. As a result, passivation of tellurium surface sites by oxygen may result in an ECL peak at a similar position with PL and no apparent PL tail.

4. Summary. In conclusion, the DPV of TOPO-capped CdTe NPs revealed the band gap of ∼2.1 eV, which was close to the optical value and two discrete anodic peaks resulting from diffusion of NPs in solution; where one large anodic peak at ∼0.7 V was proposed as a multielectron reaction. An additional anodic peak appeared because of oxidation of reduced species. The degree of stability of NPs in solution under the potential could be the main reason of the unpredicted voltammetric response. Intense ECL signal of particles was observed by electron transfer reaction between reduced NPs and reductively oxidized species of CH_2Cl_2 at negative potential region. The good correspondence of the ECL emission peak with the PL results suggests the negligible participation of surface states in the emission process. This difference with earlier ECL studies, e.g., of CdSe, perhaps results from better passivation of the tellerium surface sites in the synthesized particles.

Acknowledgment. We thank F.-R. Fan for his valuable comments and Seungwook Lee for assistance in acquiring TEM images. The support of the National Science Foundation (CHE-0202136) and the Robert A. Welch Foundation is gratefully appreciated. N.M. thanks Konkuk University for financial support in the year of 2000.

References

(1) (a) Henglein, A. *Chem. Rev.* **1989**, *89*, 1861. (b) Steigerwald, M. L.; Brus, L. E. *Acc. Chem. Res.* **1990**, *23*, 183. (c) Bawendi, M. G.; Steigerwald, M. L.; Brus, L. E. *Annu. Rev. Phys. Chem.* **1990**, *41*, 477. (d) Wang, Y.; Herron, Y. *J. Phys. Chem.* **1991**, *95*, 525. (e) Weller, H. *Adv. Mater.* **1993**, *5*, 88. (f) Weller, H. *Angew. Chem., Int. Ed. Engl.* **1993**, *32*, 41. (g) Hagfeldt, A.; Grätzel, M. *Chem. Rev.* **1995**, *95*, 49. (h) Alivisatos, A. P. *J. Phys. Chem.* **1996**, *100*, 13226.

(2) Haram, S. K.; Quinn, B. M.; Bard, A. J. *J. Am. Chem. Soc.* **2001**, *123*, 8860.

(3) (a) Ingram, R. S.; Hostetler, M. J.; Murray, R. W.; Schaaff, T. G.; Khoury, J. T.; Whetten, R. L.; Bigioni, T. P.; Guthrie, D. K.; First, P. N. *J. Am. Chem. Soc.* **1997**, *119*, 9279. (b) Chen, S.; Murray, R. W.; Feldberg, S. W. *J. Phys. Chem. B* **1998**, *102*, 9898. (c) Chen, S.; Ingram, R. S.; Hostetler, M. J.; Pietron, J. J.; Murray, R. W.; Schaaff, T. G.; Khoury, J. T.; Alvarez, M. M.; Whetten, R. L. *Science* **1998**, *280*, 2098. (d) Hicks, J. F.; Templeton A. C.; Chen, S.; Sheran, K. M.; Jasti, R.; Murray, R. W.; Debord, J.; Schaaff, T. G.; Whetten, R. L. *Anal. Chem.* **1999**, *71*, 3703. (e) Templeton, A. C.; Wuelfing, W. P.; Murray, R. W. *Acc. Chem. Res.* **2000**, *33*, 27. (f) Hicks, J. F.; Miles, D. T.; Murray, R. W. *J. Am. Chem. Soc.* **2002**, *124*, 13322. (g) Quinn, B. M.; Liljeroth, P.; Ruiz, V.; Laaksonen, T.; Kontturi, K. *J. Am. Chem. Soc.* **2003**, *125*, 6644.

(4) Ding, Z.; Quinn, B. M.; Haram, S. K.; Pell, L. E.; Korgel, B. A.; Bard, A. J. *Science* **2002**, *296*, 1293.

(5) Chen, S.; Truax, L. A.; Sommers, J. M. *Chem. Mater.* **2000**, *12*, 3864.

(6) Peng, Z. A.; Peng, X. *J. Am. Chem. Soc.* **2001**, *123*, 183.

(7) Myung, N.; Ding, Z.; Bard, A. J. *Nano Lett.* **2002**, *2*, 1315.

(8) Myung, N.; Bae, Y.; Bard, A. J. *Nano Lett.* **2003**, *3*, 1053.

(9) Zanio, K. *Semiconductors and Semimetals*, Vol. 13, Academic: New York 1978.

(10) Sahami, S.; Weaver, M. J. *J. Electroanal. Chem.* **1981**, *122*, 155.

(11) Yu, W. W.; Qu, L.; Guo, W.; Peng, X. *Chem. Mater.* **2003**, *15*, 2854.

(12) Wuister, S. F.; Swart, I.; van Driel, F.; Hickey, S. G.; de Mello Donegá, C. *Nano Lett.* **2003**, *3*, 503.

(13) Trindade, T.; O'Brien, P.; Pickett, N. L. *Chem. Mater.* **2001**, *13*, 3843.

(14) Gao, M.; Sun, J.; Dulkeith, E.; Gaponik, N.; Lemmer, U.; Feldmann, J. *Langmuir* **2002**, *18*, 4098.

(15) Greene, I. A.; Wu, F.; Zhang, J. Z.; Chen, S. *J. Phys. Chem. B* **2003**, *107*, 5733.

(16) Kolosky, M.; Vialle, J.; Cotel, T. *J. Chromatogr.* **1984**, *299*, 436.

(17) Bard, A. J.; Santhanam, K. S. V.; Cruser, S. A.; Faulkner, L. R. In *Fluorescence: Thoery, Instrumentation, and Practice*; Guilbault, G. G., Ed.; Marcel Dekker: New York, 1967.

(18) Ushida, K.; Yoshida, Y.; Kozawa, T.; Tagawa, S.; Kira, A. *J. Phys. Chem. A* **1999**, *103*, 4680.

(19) Faulkner, L. R.; Bard, A. J. In *Electroanalytical Chemistry*; Bard, A. J., Ed.; Marcel Dekker: New York, 1977; Vol. 10.

(20) Becerra, L. R.; Murray, C. B.; Griffin, R. G.; Bawendi, M. G. *J. Chem. Phys.* **1994**, *100*, 3297.

(21) Katari, J. E. B.; Colvin, V. L.; Alivisatos, A. P. *J. Phys. Chem.* **1994**, *98*, 4109.

(22) Borchert, H.; Talapin, D. V.; Gaponik, N.; McGinley, C.; Adam, S.; Lobo, A.; Möller, T.; Weller, H. *J. Phys. Chem. B* **2003**, *107*, 9662.

(23) Bard, A. J.; Faulkner, L. R. In *Electrochemical Methods: Fundamentals and Applications*, 2nd ed.; John Wiley & Sons: New York, 2001; p 290.

(24) VisWanath, D. S.; Natarajan, G. *Data Book on the Viscosity of Liquids*; Hemisphere Publishing Corp.: New York, 1989.

(25) Jiang, J.; Krauss, T. D.; Brus, L. E. *J. Phys. Chem. B* **2000**, *104*, 11936.

NL049516X